Am. J. Hum. Genet. 63:1732–1742, 1998

Vocal Cord and Pharyngeal Weakness with Autosomal Dominant Distal Myopathy: Clinical Description and Gene Localization to 5q31

Howard Feit,[1] Alice Silbergleit,[1] Lori B. Schneider,[1] Jorge A. Gutierrez,[2] Reine-Paule Fitoussi,[4] Cécile Réyès,[4] Guy A. Rouleau,[5] Bernard Brais,[5] Charles E. Jackson,[3] Jacques S. Beckmann,[4] and Eric Seboun[4]

Departments of [1]Neurology, [2]Pathology, and [3]Genetics, Henry Ford Hospital, Detroit; [4]CNRS-URA 1922/Généthon Laboratory, Evry, France; and [5]Centre for Research in Neurosciences, McGill University, Montreal General Hospital, Montreal

Summary

Distal myopathy refers to a heterogeneous group of disorders in which the initial manifestations are weakness and atrophy of the hands and feet. We report a family segregating an autosomal dominant distal myopathy, with multiple affected individuals in whom vocal cord and pharyngeal weakness may accompany the distal myopathy, without involvement of the ocular muscles. To our knowledge, this pedigree displays a distinct distal myopathy with the added features of pharyngeal and vocal cord dysfunction (VCPDM) that has not been previously reported. We mapped the *MPD2* gene for VCPDM to chromosome 5q within a 12-cM linkage interval between markers D5S458 and D5S1972 in a large pedigree (a maximum LOD score of 12.94 at a recombination fraction of 0 for D5S393) and combined genome screening and DNA pooling successfully adapted to fluorescent markers. This technique provides for the possibility of fully automated genome scans.

Introduction

Distal myopathy refers to a heterogeneous group of disorders in which the initial manifestations are weakness and atrophy of the hands and feet (Griggs and Markesbery 1994). The inheritance can be dominant or recessive, for both childhood- and adult-onset forms. In some distal myopathies, the muscle biopsy may display a rimmed vacuolar myopathy with trichrome stains. There are some autosomal dominant distal myopathies that display inclusion bodies (Askanas and Engel 1998; Fardeau and Tome 1998). We report a family segregating an autosomal dominant distal myopathy, with multiple affected individuals in whom vocal cord and pharyngeal weakness may accompany the distal myopathy, without involvement of the ocular muscles. This form of distal myopathy has not been previously recognized and is distinct from other myopathies with pharyngeal or vocal weakness. We localized the gene responsible for this disorder to chromosome 5q31 by combining genome screening and DNA-pooling strategies that use fluorescent microsatellite markers.

Received August 5, 1998; accepted for publication October 12, 1998; electronically published November 10, 1998.

Address for correspondence and reprints: Dr. Eric Seboun, CNRS-URA 1922/Généthon, 1 Rue de l'Internationale, 91002 Evry, France. E-mail: seboun@genethon.fr

0002-9297/98/6306-0020$02.00

Family and Methods

Family Collection

The study was approved by the review board of the Henry Ford Hospital. Informed consent was obtained from family members.

DNA Isolation, Pooling, and Genotyping

DNA was isolated and purified from peripheral blood by use of standard protocols. We adapted the DNA-pooling genome-scanning method (Sheffield et al. 1994; Carmi et al. 1995) to fluorescent markers. Two DNA pools, one for the healthy individuals and one for the affected members, were prepared. DNA concentration was determined by optical density (OD) reading at 260 nm. DNA concentration was set to 100 μg/ml before pooling. DNA quality and concentration were controlled by PCR amplification. Each pool was made by the combination of seven DNA samples. After pooling, DNA concentration was checked to be ~100 μg/ml by use of OD reading. Because age at onset for the disease initially appeared to be 35–57 years, the pool of healthy individuals was prepared with DNA from unaffected members >57 years of age.

Genotyping was performed with fluorescent end-labeled microsatellite markers from the Généthon map; average spacing was 15 cM. PCR reactions were per-

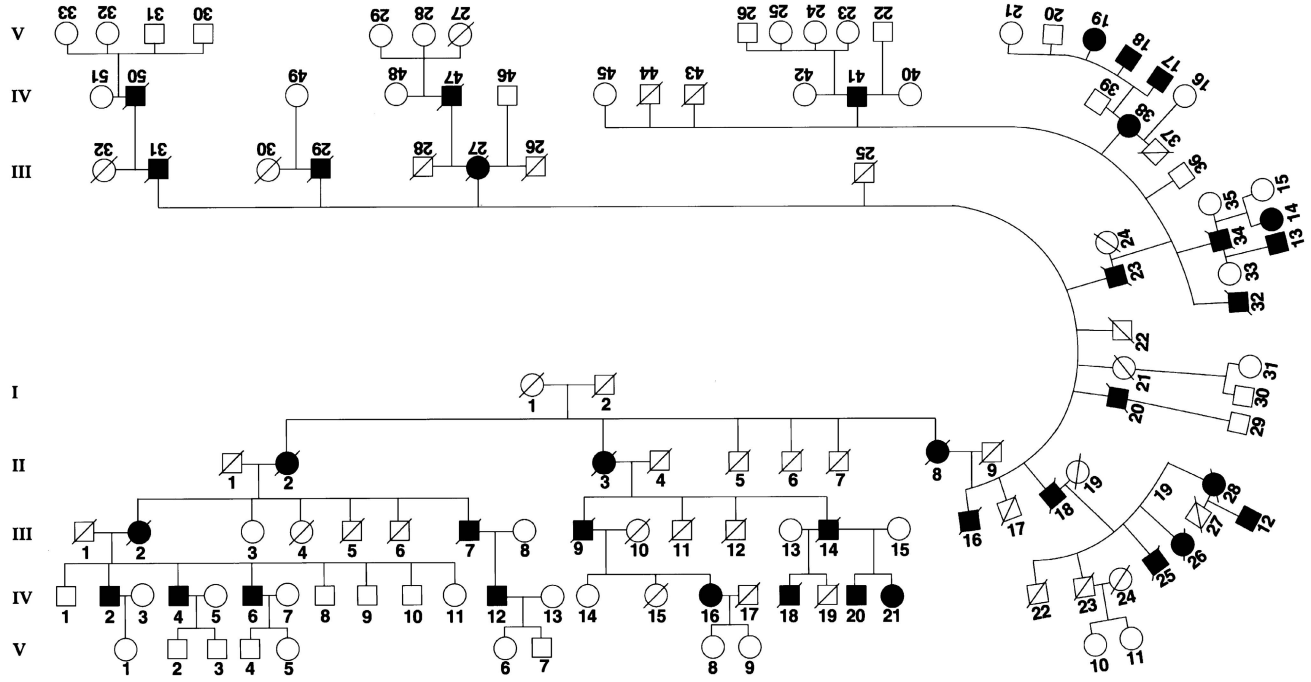

Figure 1 Pedigree of the initial branch of the kindred studied. Blackened circles and squares indicate members reported to be affected or definitely affected, determined on the basis of neurological findings.

formed in 15 μl containing 20 ng genomic DNA, 0.33 mM each primer, 0.16 mM dNTPs, 10 mM Tris-HCl, pH 9, 50 mM KCl, 1.5 mM $MgCl_2$, 0.1% Triton, and 0.5 U *Taq* polymerase. DNA was denatured for 5 min at 96°C followed by 35 cycles of amplification (denaturation for 40 s at 94°C, and annealing and elongation for 30 s at 55°C). After the last cycle of amplification, ends were repaired by the incubation of the PCR products for 30 min at 37°C, with 0.3 U T4 DNA polymerase. PCR products were combined by series of 8–12, dependent on fluorophore and expected allele size. Aliquots were denatured for 5 min at 94°C before being loaded onto a 5% denaturing polyacrylamide gel (Vignal et al. 1993). Alleles were separated by electrophoresis performed with 373 ABI sequencers. Genotyping data were processed with GENOTYPER (ABI), GENSCAN (ABI), and MARKSYN (Généthon) softwares.

Statistical Analysis of Linkage Data

LOD-score analysis was computed by use of FASTLINK (Schaffer 1996), under a dominant mode of inheritance and isofrequent alleles. The frequency of the disease allele was set to .0001. Age-dependent penetrance was evaluated by use of the affected members of the family.

Haplotypes were constructed by use of GENEHUNTER (Kruglyak et al. 1996). Because of the size of the family and computation time limits, the pedigree was broken into overlapping subfamilies, to ensure fast and consistent haplotype construction.

Results

Clinical Features

The family's pedigree is shown in figure 1, and the clinical features of 12 affected individuals are summarized in table 1. The family is Caucasian and originates from the vicinity of southeastern Tennessee. Twelve of 37 reportedly affected individuals were examined clinically. An autosomal dominant inheritance is likely in this four-generation pedigree. The typical age at onset is 35–57 years (average 45.7 years). The muscle weakness usually involves the feet and ankles first but may start in the hands. In two individuals (V-13 and V-14), voice change was the initial manifestation. Asymmetric involvement at onset is very typical, but eventually a symmetric distal weakness of the hands and legs prevails. The weakness in the legs often has a peroneal distribution, but it eventually involves inversion of the ankle, rendering the gait very unstable. The gastrocnemius muscle is usually relatively spared. The use of ankle-foot orthotic braces and/or canes may become necessary, but ambulation is generally preserved. In the hands, the pattern of weakness is very characteristic. The extensors of

Table 1

Clinical Features of 12 Affected Individuals in the Kindred

Individual	Current Age (years)	Age at Onset (years)	Sex	Distal Weakness	Shoulder Weakness	Swallowing or Vocal Dysfunction	CPK (× Normal)
IV-2	56	45	M	L leg* > R R hand = L	R > L	+	2 (45)
IV-4	48	44	M	R hand* > L R leg = L	R	+	WNL (45)
IV-6	65	57	M	L leg* > R	…	+	WNL
IV-12	50	45	M	R leg* > L R hand > L	…	+	1.3 (45)
IV-52	60	48	M	R leg* > L L hand > R	…	…	2
IV-38	72	54	F	Hands* Legs	R > L	+	WNL
V-12	51	40	M	Legs* R hand = L	…	+	2
V-13	42	41	M	R leg = L R hand	…	+*	2
V-14	58	52	F	Hands = legs	…	+*	…
V-17	52	35	M	L leg* > R R hand = L	R = L	…	2
V-18	50	35	M	R leg* > L	…	…	8
V-19	47	47	F	Hands Legs	…	+	WNL

NOTE.—An asterisk (*) indicates the first symptom. CPK values are listed in relation to the upper limits of normal for the particular laboratory. If the CPK value was obtained at an age differing from the current age, then that age (in years) is given in parentheses. WNL = within normal limits.

the fingers are each affected to a varying degree. If the hand is placed on a table, some fingers can be lifted whereas others cannot. The variable weakness affects the position of the fingers differently when the patient is asked to extend the fingers and wrist (Brooke 1986). The initial weakness in the hand also selectively involves the abductor pollicis brevis, which is often strikingly atrophied but without other symptoms of median nerve entrapment.

The vocal cord and pharyngeal weakness can be present at the onset of the distal-extremity weakness. At first, the voice has a hypophonic, breathy quality, but this may slowly progress to a wet, gurgling, hoarse voice with hypernasal resonance and difficulty with swallowing and aspiration. Activities such as gargling become impossible. In some cases, laryngoscopy reveals bowing of the vocal cords, with secretions constantly flowing past as a result of incomplete closure of the glottis and pharyngeal muscle weakness. The vocal cords can be voluntarily opened but will never close properly. Aspiration may be reduced by the injection of agents that add bulk and act as stiffeners (teflon, gel foam, or fat) or by bilateral silastic-implant medializations of the vocal folds. Vocal cord dysfunction or swallowing disorder was present in 9 of 12 affected individuals and was reported to have occured in most of the affected deceased relatives, at older ages.

Shoulder weakness was the only proximal muscle involvement noted. The weakness was usually asymmetric and predominantly affected the deltoid. Four of 12 individuals had shoulder weakness. Progressive external ophthalmoplegia was not found. Significant ptosis was not noted, except in one individual (IV-38) who reported ptosis requiring corrective surgery at age 43 years. One patient (V-12) was oxygen-dependent with restrictive pulmonary disease and left-ventricular dysfunction with ejection fraction of 45%. One patient (IV-50) was reported to have cardiomyopathy together with coronary artery disease. Frank unexplained cardiomyopathy was not observed.

Electrodiagnostic and Muscle Biopsy Studies

Electromyographic (EMG) and nerve conduction–velocity (NCV) data were available for 7 of 12 individuals (table 2). The compound–muscle action potentials in limb muscles could be either myopathic or neuropathic. In 3 of 7 individuals, the NCV was mildly or borderline slow. Electrodiagnostic studies of the vocal and pharyngeal muscles in two individuals (IV-6 and IV-12) showed myopathic potentials (table 3).

Muscle biopsy was performed on 6 of 12 individuals. Patient IV-6 had quadriceps and gastrocnemius biopsies that disclosed a chronic noninflammatory myopathy

Table 2

EMG, NCV, and Muscle-Biopsy Data on Seven Affected Members of the First Branch of the Kindred

Individual	EMG	NCV	Muscle Biopsy
IV-2	Myopathy	Normal	Rimmed vacuoles, central nuclei
IV-6	Distal denervation	Normal	Rimmed vacuoles, atrophy
IV-38	Myopathy	Borderline slow	End-stage myopathy
IV-52	Neuropathy	Slow	…
V-12	Myopathy	Slow	Rimmed vacuoles, thin myelin
V-13	Neuropathy	…	Rimmed vacuoles, central nuclei
V-14	Myopathy	Normal	Rimmed vacuoles, central nuclei

with the presence of characteristic, usually subsarcolemmal, rimmed vacuoles. In addition, there were atrophic fibers consistent with denervation. The pathologic changes were scant in the quadriceps and severe in the gastrocnemius. Individual V-13 had a gastrocnemius biopsy that demonstrated a slight to moderate noninflammatory myopathy with rimmed vacuoles and that also had occasional atrophic fibers suggestive of denervation. Ultrastructural studies of subject showed sparse, small tubular aggregates close to the triads and occasionally associated with minute myelinoid figures. In these biopsies (IV-6 and V-13) thorough enzyme histochemical (NADH, succinate dehydrogenase/phenazine metholsulfonate, cytochrome C oxydase, nonspecific esterase, alkaline phosphatase, and ATPase at pHs 9.4, 4.6, and 4.3) and ultrastructural (two grids per case) studies failed to demonstrate mitochondrial abnormalities, amyloid deposits (Congo red), or filamentous inclusions. In a third patient (V-14), light (H and E, trichrome, NADH, and ATPase) and electron-microscopy studies of a biopsy from an unspecified muscle disclosed a mild, noninflammatory myopathy with rimmed vacuoles; the muscle was devoid of sarcoplasmic or intranuclear inclusions, amyloid deposits (thioflavin T), or filamentous inclusions (Tome and Fardeau 1994). The muscle biopsies of two other individuals (IV-2 and IV-12) were reported to show that of rimmed vacuoles, and a third subject (IV-38) showed end-stage myopathy. One individual (V-12) underwent a sural nerve biopsy in which thinned myelin sheaths were reported.

Creatine phosphokinase (CPK) serum levels were generally within twice the upper limits of normal (table 1). No values above twice-normal were encountered in younger unaffected but at-risk members of the family. These findings are probably related to the slow progression of the disease and to the relatively small mass of muscle involved.

DNA Pooling with Fluorescent Markers

At first, linkage to the oculopharyngeal muscular dystrophy (OPMD; MIM 164300) locus on 14q was excluded by use of the two closest flanking markers (data not shown; Brais et al. 1998). As a result, to map the distal myopathy with the vocal cord and pharyngeal weakness (VCPDM) gene a genomewide search was undertaken at Généthon. To reduce the genotyping effort, the genome scan was done by means of DNA pooling (Sheffield et al. 1994; Carmi et al. 1995). We adapted this strategy to fluorescent markers. Several recessive disorders have been successfully mapped by DNA pooling in consanguineous families. To date, only one dominantly inherited disease has been localized by use of such a strategy (Brugada et al. 1997). In this approach, the implicit hypothesis of a founder effect and a skewed marker-allele distribution between the affected- and healthy-individual DNA pools is anticipated for markers in the vicinity of the disease gene. This approach fitted perfectly the analysis of our large pedigree. Although in recessive disorders homozygosity by descent inherited from a common ancestor is expected at the disease locus, in this case we expected skewing of a single allele.

A DNA pool was prepared by the combination of the DNA from seven affected members. A control DNA pool was comprised from seven healthy individuals. Because the age at disease onset is 35–57 years, the pool of healthy individuals was prepared by selection of the oldest unaffected members of the family. Pools were genotyped with fluorescent end-labeled microsatellite markers from the Généthon map (Weissenbach et al. 1992; Dib et al. 1996). Average spacing was 15 cM. The genome scan demonstrated that two markers, D5S393 and D5S410, located on the long arm of chromosome 5 and separated by 21 cM, showed a marked difference in allele distribution between the two pools. These findings suggested possible linkage (fig. 2). The most dramatic effect was observed for D5S393. The 170-bp allele was almost totally absent from the "healthy" DNA pool, whereas it was quite frequent in the "affected" DNA pool. Likewise, the representation of the 162-bp allele was increased in the "healthy" DNA pool and decreased in the "affected" DNA pool. Although not as striking

Table 3

EMG Study Results on Vocal and Pharyngeal Muscles of Two Affected Members

Muscle	IV-6	IV-12
Palatopharyngeus	Myopathic	Myopathic
Cricothyroideus	Normal	Normal
Strapedius	Normal	Normal
Vocalis	Myopathic	Myopathic
Cricopharyngeal	Myopathic	Myopathic

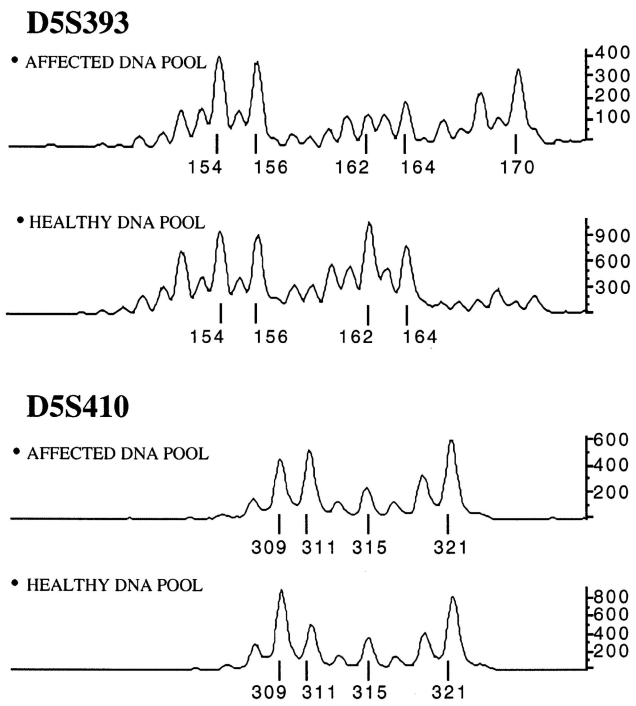

Figure 2 Allele frequency and distribution for DNA markers on 5q. DNA pools were prepared by the combination of DNA from seven affected members ("affected DNA pool") and from the oldest unaffected members ("healthy DNA pool") of the family. Pools were genotyped with fluorescent end-labeled microsatellite markers from the Généthon map, on an ABI 373. Average spacing is 15 cM. The allele sizes (in bp) are indicated below the peaks. Fluorescence intensity was measured at the peaks by use of the ladder on the right.

as that for D5S393, a skewed distribution between both pools for the 309- and 311-bp alleles of D5S410 was also observed. This study suggested that the VCPDM gene might be located between these two markers.

Two-Point Linkage Analysis

The 12 affected members of the initial family were genotyped for D5S393 and D5S410. Linkage was evaluated by the LOD-score method. Two-point linkage analysis was performed under a dominant model. Evidence of linkage was obtained for D5S393 with a maximum LOD score (Z_{max}) of 5.16 at a recombination fraction (θ) of .05. D5S410 gave a LOD score of 0.6 at $\theta = .3$. These results were consistent with the pooling data.

During this study, one member of the family identified another, new branch, descended from the sister of I-1 (fig. 1). This branch contains seven living affected members from whom DNA was obtained. These new members were genotyped for 14 markers, including D5S393 and D5S410, in accordance with a standard protocol (Vignal et al. 1993). Two markers were located proximal to D5S393, and 10 markers spanned the 21-cM region between D5S393 and D5S410. Two-point linkage analysis was performed under a dominant model with age-dependent penetrance and isofrequent alleles (table 4). Results confirmed linkage, with $Z_{max} = 12.94$ at $\theta = .0$ for D5S393, by use of isofrequent alleles ($f = .09$). This LOD score was very close to the expected LOD score (12.98 at $\theta = .00$) obtained by linkage simulations for a marker with five isofrequent alleles (Ott 1989; Weeks et al. 1990). Because the LOD score depends on the allele frequency, we varied the allele frequency for the allele present on the disease haplotype, while keeping the other alleles isofrequent. By use of frequencies of .01 and .3, LOD scores of 15.85 and 8.99, respectively, were obtained.

Fine Mapping of the VCPDM Gene

Fine mapping of the VCPDM gene was undertaken by haplotype construction and identification of recombinant haplotypes, by use of genotyping data for the 14 markers that span the region of interest (fig. 3). A total of 21 affected individuals were studied, and several recombinant haplotypes were identified. Results from four affected individuals, each of whom represent a class of recombinant haplotypes, are presented in figure 4. The centromeric recombination point was defined by D5S1995 for member V-37. The telomeric recombination point was defined by D5S436 for member V-14.

Table 4

Two-Point Linkage Analysis Data, Determined by Use of an Autosomal Dominant Model with Age-Dependent Penetrance and Even Marker-Allele Frequencies

	Recombination fraction at $\theta =$						
Marker	.00	.1	.2	.3	.4	Z_{max}	θ_{max}
D5S1995	6.12	7.95	6.17	4.08	1.90	8.69	.026
D5S458	7.42	5.98	4.32	2.54	.82	7.42	.000
D5S393	12.94	10.74	8.23	5.46	2.54	12.94	.000
D5S479	10.73	8.81	6.64	4.29	1.89	10.73	.000
D5S414	10.52	8.66	6.49	4.10	1.64	10.52	.000
D5S500	8.79	7.37	5.66	3.75	1.76	8.79	.000
D5S658	8.70	7.57	5.94	3.99	1.87	8.69	.000
D5S2011	6.17	4.91	3.55	2.17	.92	6.17	.000
D5S2017	5.29	4.31	3.15	1.94	.83	5.29	.000
D5S1972	5.18	4.59	3.53	2.26	.99	5.18	.000
D5S436	−5.29	6.05	5.11	3.53	1.67	6.09	.081
D5S638	−6.88	2.71	2.45	1.70	.80	2.73	.117
D5S2090	−10.54	3.27	2.92	1.95	.81	3.29	.116
D5S410	−22.93	.46	1.24	1.01	.45	1.24	.212

Note.—LOD scores were computed by FASTLINK (Schaffer 1996), under a dominant mode of inheritance and even allele frequencies. The frequency of the disease allele was set to .0001. The age-dependent penetrance plot was constructed mainly from the patients examined and on the basis of information from other neurologists' reports and from what appeared to be reliable family memories of the onset of the disease in their affected close relatives now deceased.

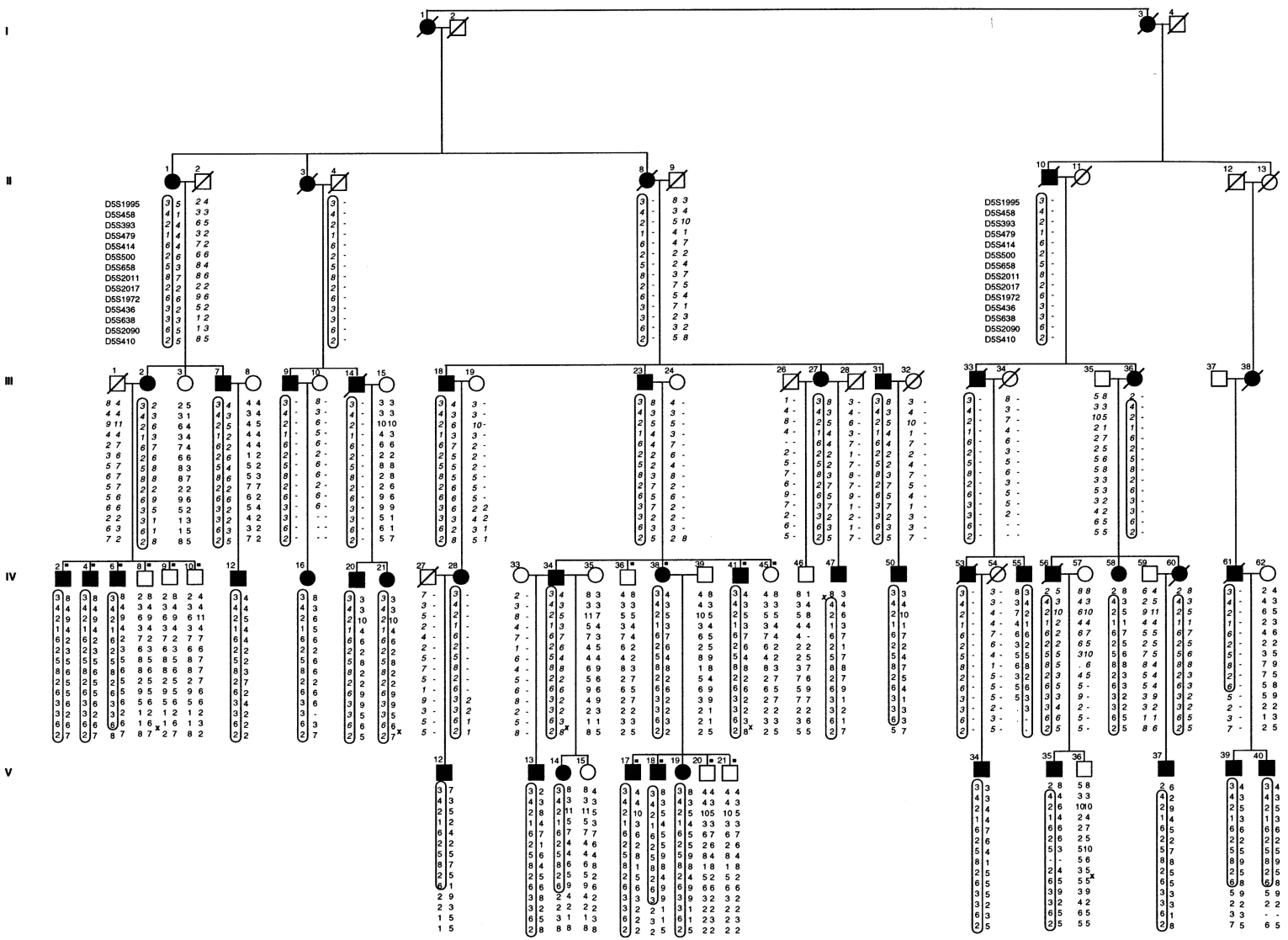

Figure 3 Haplotypes of 14 DNA markers on 5q in affected members from both branches of the kindred. DNA samples used in the DNA-pooling strategy are indicated by tiny blackened squares next to the member number. Haplotypes were inferred by use of GENEHUNTER (Kruglyak et al. 1996). Reconstructed haplotypes are in italic type. To ensure fast and consistent haplotype construction, the pedigree was broken into overlapping subfamilies. The disease haplotype is circled.

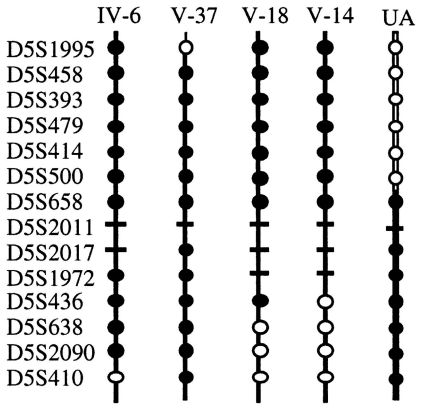

Figure 4 Illustration of the haplotypes of one unaffected and four affected individuals, depicting recombination regions. Schematic representation of the chromosomes shows specific recombination events relevant to the localization of the *MPD2* gene. Fourteen markers are shown; the order is based on the Généthon linkage map. The unaffected (UA) and the affected (IV-6, V-37, V-18, and V-14) members were used to define the smallest linkage interval and are indicated above the haplotype. Circles indicate informative meioses. Parental alleles segregating with the disease or the normal allele are represented, by blackened or unblackened circles respectively. Horizontal bars indicate uninformative meioses.

However, D5S1972 and the two proximal markers, D5S2011 and D5S2017, were not informative, and the recombination may have occurred anywhere between D5S658 and any of these three markers. To better map the recombination point, two additional markers located within this interval were typed but turned out to be uninformative (data not shown). On the basis of the results from the affected members, the chromosomal region linked to the VCPDM gene was determined to be between markers D5S436 and D5S1995 and to span a 12-cM region (fig. 5).

A 49-year-old healthy member (UA) carried a recombinant disease haplotype (fig. 4). If this individual carried the disease haplotype, UA would have a 70% chance of the disease being evident at this age. The negative examination suggested the presence of a preferential location of the disease gene, within the D5S1995–D5S658 linkage interval.

Discussion

We mapped the gene for VCPDM to chromosome 5q, within a 12-cM linkage interval between markers D5S458 and D5S1972 by genome screening using the DNA-pooling strategy in a large pedigree. Linkage to this locus is supported by a $Z_{max} = 12.94$ at $\theta = 0$ for marker D5S393 and by the presence of a shared disease haplotype among all affected members. The potential recombinant seen in one unaffected member of this family (UA, fig. 4) suggests that the VCPDM gene maps within the proximal part of the 12-cM interval. This data inference is in agreement with the location suggested by the confidence interval (not shown) calculated under the assumption of isofrequent allele distribution. Altogether, this may restrict the interval to D5S1995–D5S658, a 7-cM region.

DNA pooling has proved to be a very efficient and successful way to map genes mainly for recessive disorders in consanguineous families (Sheffield et al. 1994; Carmi et al. 1995). One dominantly inherited disorder (Brugada et al. 1997) was mapped by pooling, and feasibility was assessed, by use of fluorescent markers, for two diseases for which gene locations were known (Damji et al. 1998). We successfully adapted this strategy to fluorescent markers and showed its potential in combining genome screening and DNA pooling. This technique provides for the possibility of fully automated genome scans. Slippage of the T4 DNA polymerase during PCR amplification usually produces shorter artifactual DNA fragments, which could interfere with allele reading in DNA pools. In our situation, the allele found in the DNA pool of the affected members, for D5S393,

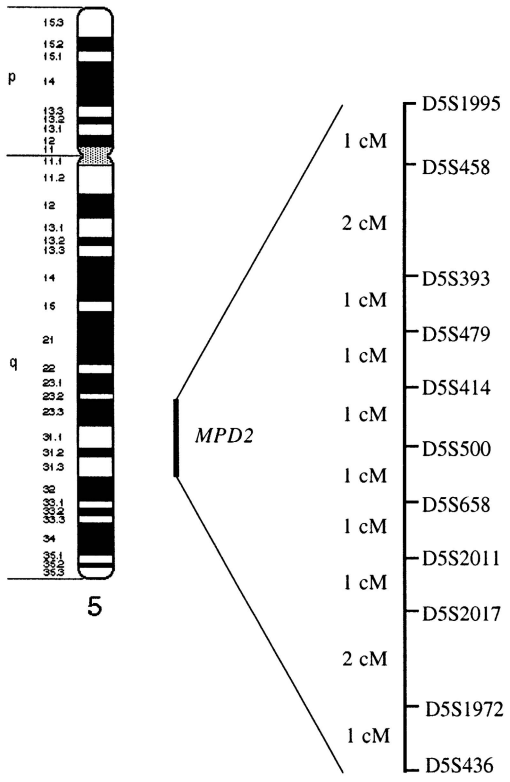

Figure 5 Schematic representation of chromosome 5q31 area linked to the *MPD2* locus. Distance between markers is indicated in centimorgans, in accordance with the Généthon linkage map. Cytogenetic location is based on the Human Gene Map.

Table 5

List of Classical Distal Myopathies

Designation	Inheritance[a]	Key Clinical Features	Gene Location
Welander myopathy[b]	AD	Late adult onset in hands	Unknown
Tibial muscular dystrophy[b]	AD	Late adult onset in anterior tibial muscles	2q31[c]
Markesbery-Griggs	AD	Late adult onset in distal limbs, eventual proximal involvement	Unknown
Miyoshi myopathy	AR	Early adult onset in gastrocnemius muscles	2p12 [d]
Nonaka myopathy	AR	Early adult onset in distal anterior leg muscles	9[e]
Distal myopathy[f]	AD	Onset at 4–25 years, in toe, ankle, finger extensors, neck flexors	14
VCPDM[g]	AD	Late adult onset in ankle or finger extensors; vocal/pharyngeal weakness	5q31[g]

NOTE.—From Griggs and Markesbery 1994.

[a] AD = autosomal dominant, and AR = autosomal recessive.

[b] Also see review chapters in Askanas et al. 1998.

[c] Haravuori et al. 1998.

[d] Bejaoui et al. 1995.

[e] Ikeuchi et al. 1997.

[f] Laing et al. 1995.

[g] This report.

had a size (170 bp) very distinct from that of all the other alleles observed in the pool, and slippage did not blur the result. Even for D5S410, the skewed distribution between both pools concerning two alleles with a 2-bp difference (309 bp and 311 bp) was quite visible. Deconvolution methods that mathematically remove PCR-slippage artifacts (Perlin et al. 1995) could improve genotyping accuracy, particularly in DNA pooling.

To our knowledge, this pedigree displays a distinct form of VCPDM that has not been previously reported (table 1). Inherited myopathies with important laryngeal/pharyngeal weakness include OPMD and oculopharyngodistal myopathy (Tome and Fardeau 1994); however, our patients did not have significant ptosis (with one exception) or progressive external ophthalmoparesis. Although proximal weakness is more common in OPMD, distal weakness has been reported in both OPMD and oculopharyngodistal myopathy. The disorder that we report can be distinguished from OPMD by the lack of ocular-muscle involvement and the absence of intranuclear filamentous inclusions on electron microscopy of the three patients studied. Furthermore, linkage studies exclude the 14q11 OPMD locus in our family. Oculopharyngodistal myopathy is characterized by slowly progressive ptosis, ophthalmoparesis, dysphagia, and distal weakness (Fardeau and Tome 1998). It is uncertain whether oculopharyngodistal myopathy is a variant of OPMD with distal weakness or a distinct myopathy. It is possible that our family represents a variant of oculopharyngodistal myopathy without the ocular involvement and with a later age at onset. Additional linkage studies will help distinguish these disorders.

From a histopathological standpoint, the lesion observed in these individuals with a noninflammatory myopathy with rimmed vacuoles probably fits into the spectrum of the inclusion-body myopathies. Overall, the myopathy was mild or moderate. In one patient, the myopathy was very subtle in the quadriceps but moderate to severe in the gastrocnemius, where it had a dystrophic pattern. A finding that was present in all specimens was rimmed vacuoles, with a characteristic light electron-microscopy appearance. In the three biopsies studied ultrastructurally, questionable sarcoplasmic filaments were observed in only one case. In these biopsies, amyloid was not detected by histochemical stains. However, in a given case, filaments may be scant, and their identification may be difficult. Furthermore, immunohistochemistry for β-amyloid or for paired helical filaments was not performed on any of the biopsies. Although morphologically this rimmed vacuolar myopathy cannot be separated from the Swedish, Finnish, and other autosomal dominant inclusion-body myopathies (Askanas and Engel 1998), its characteristic distal/vocal cord/pharyngeal involvement and genetic abnormality indicate that it is a separate clinicopathologic entity.

The autosomal dominant distal myopathies are a heterogeneous group of disorders that tentatively can be classified by age at onset and by the characteristic that muscles typically are involved first (table 5). More recent linkage studies have helped to further distinguish these disorders (table 5). The phenotype that we describe differs from the other autosomal dominant distal myopathies in that the weakness can start in the hands, feet, or voice/pharynx. The weakness in the hands involves the finger extensors and abductor pollicis brevis muscles, which is different from the thumb and index-finger weakness of the Scandinavian form of distal myopathy. The neck flexors were not involved in our patients (both clinically and with electrodiagnostic testing), even when there was severe vocal and pharyngeal weakness; this differs from the patients of Laing et al. (1995), who had *MPD1* distal myopathy. In addition, the weakness does not remain confined to the ankle extensors, as in tibial

muscular dystrophy. The assignment of this disorder to a locus on chromosome 5q also distinguishes this disorder from other forms of dominantly inherited distal myopathy. In keeping with the precedent started by Laing et al. (1995), the gene on 5q for this form of distal myopathy is designated *"MPD2."*

The phenotype that we describe in this family closely resembles that reported by Young and Harper (1980) as an autosomal dominant distal atrophy with vocal cord paralysis. In the family reported by Young and Harper, EMGs were obtained for two of nine affected individuals and showed spontaneous fibrillation and either "reduced interference pattern" or "reduced volitional activity." Muscle biopsies were not obtained. In our family, both neurogenic and myopathic muscle potentials were observed. Thus, we cannot exclude the possibility that the phenotype reported by Young and Harper (1980) as a distal atrophy with vocal cord paralysis was possibly a distal myopathy instead. Linkage studies of the families reported by Young and Harper (1980) may clarify this issue. The *MPD2* phenotype is also easily confused with the neuronal form of Charcot-Marie-Tooth disease if the EMG results for an individual patient suggest a neurogenic disorder with normal conduction velocities. The diagnosis of VCPDM does not require voice and pharyngeal changes, since some affected individuals in our kindred did not show these changes at the time of their examinations. Attention to the presentation and subsequent course in other family members is important. Muscle biopsies that include an involved distal muscle and examinations of other affected members of the family are recommended.

Two diseases have been mapped to this chromosomal region: an autosomal recessive (LGMD2F; MIM 601287) and an autosomal dominant (LGMD1A; MIM 15900) limb-girdle muscular dystrophy. LGMD2F has been mapped to chromosome 5q33-34 (Passos-Bueno et al. 1996) and is a result of a mutation in the δ-sarcoglycan gene (Nigro et al. 1996). This gene is telomeric to the linkage interval we defined and is therefore excluded. LGMD1A has been mapped within a 2.5-Mb interval flanked by D5S479 and D5S594 (Bartoloni et al. 1997). Our linkage interval encompasses the LGMD1A locus; however, both disorders are clinically quite different. The proximal weakness in LGMD1A is always much more severe than the distal weakness; the opposite is observed in VCPDM. Age at onset is earlier in LGMD1A, and anticipation is also suspected (Speer et al. 1998). In contrast, there is no evidence of anticipation in VCPDM. Both diseases could actually be caused by distinct mutations affecting either the same gene or syntenic genes. At this point, these hypotheses cannot be resolved. It should be remembered that both studies were based on the examination of a single large family that represents a founder effect and in which a single pathogenic mutation is segregating. Hence, it is difficult at this stage to generalize the clinical description to other mutations within these genes. It will be of interest to review the clinical properties once other independent VCPDM and LGMD1A families have been identified. A similar situation has been observed for LGMD2B (LGMD2B; MIM 253601) and the distal Miyoshi type of muscular dystrophy (ARDMD; MIM 254130), which both mapped to chromosome 2p (Bashir et al. 1994; Bejaoui et al. 1995). Recent results have shown that both diseases segregated in the same family, which suggests that they were both a result of the same allele (Illarioshkin et al. 1996; Weiler et al. 1996).

The protein coded by the autosomal dominant gene for VCPDM is unknown but is presumed to be expressed in skeletal muscle. A search of the Human Gene Map database for the D5S1995–D5S658 linkage interval revealed 161 expressed sequence tags (ESTs) with no known function in most instances. Among the ESTs with a putative or known function, one (locus HSRNASMAP; European Molecular Biology Library accession number X87613) codes for a putative transcription factor that contains a bromodomain highly expressed in skeletal muscle (Nielsen et al. 1996). This gene is located between D5S393 and D5S500 and represents a potential candidate gene. An autosomal dominant form of progressive hearing loss (DFNA15; MIM 602459) results from an 8-bp deletion in the transcription factor POU4F3 (Vahava et al. 1998). POU4F3 is located on chromosome 5q31 telomeric to the VCPDM linkage interval. In OPMD, the trinucleotide $(GCG)_{8-13}$, coding for a polyalanine tract is amplified in the poly(A)-binding protein 2 gene (*PABP2*) on chromosome 14q. The PABP2 protein is highly expressed in the nuclei of skeletal-muscle fibers (Brais et al. 1998). HSRNASMAP therefore represents a good candidate gene for VCPDM. Its possible role in VCPDM is presently being investigated.

Acknowledgments

We would like to thank Dr. Michael S. Benninger (Otolaryngology Department, Henry Ford Hospital, Detroit), Cindy Grywalski, Ralph Thompson, the patients and their family; and the many physicians who provided clinical data. C.E.J. and E.S. were supported by grants from l'Association Française contre les Myopathies.

Electronic-Database Information

Accession numbers and URLs for data in this article are as follows:

Généthon, http://www.genethon.fr (for fluorescent end-labeled microsatellite markers and GENOTYPER (ABI), GENSCAN (ABI), and MARKSYN software)

Human Gene Map Database, http://www.ncbi.nlm.nih.gov/SCIENCE96/ (for ESTs in D5S1995–D5S658 interval)

Online Mendelian Inheritance in Man (OMIM), http://www.ncbi.nlm.nih.gov/Omim/ (for OPMD [MIM 164300], LGMD2F [MIM 601287], LGMD1A [MIM 15900], LGMD2B [MIM 253601], ARDMD [MIM 254130], and DFNA15 [MIM 602459])

References

Askanas V, Engel WK (1998) Newest approaches to diagnosis and pathogenesis of sporadic inclusion-body myositis and hereditary inclusion-body myopathies, including molecular-pathologic similarities to Alzheimer disease. In: Askanas V, Serratrice G, Engel WK (eds) Inclusion-body myositis and myopathies. Cambridge University Press, Cambridge, pp 3–78

Askanas V, Serratrice G, Engel WK (eds) (1998) Inclusion-body myositis and myopathies. Cambridge University Press, Cambridge

Bartoloni L, Horrigan SK, Zhang Y, Viles K, Gilchrist JM, Vance JM, Yamaoka LH, et al (1997) Limb-girdle muscular dystrophy 1A: refinement of the 5q31 localization and a physical and genetic map of the interval. Am J Hum Genet Suppl 61:A267

Bashir R, Strachan T, Keers S, Stephenson A, Mahjneh I, Marconi G, Nashef L, et al (1994) A gene for autosomal recessive limb-girdle muscular dystrophy maps to chromosome 2p. Hum Mol Genet 3:455–457

Bejaoui K, Hirabayashi K, Hentati F, Haines JL, Ben Hamida C, Belal S, Miller RG, et al (1995) Linkage of Miyoshi myopathy (distal autosomal recessive muscular dystrophy) to chromosome 2p12. Neurology 45:768–772

Brais B, Bouchard JP, Xie YG, Rochefort DL, Chretien N, Tome FM, Lafreniere RG, et al (1998) Short GCG expansions in the PABP2 gene cause oculopharyngeal muscular dystrophy. Nat Genet 18:164–167

Brooke MH (1986) A clinician's view of neuromuscular diseases. Williams & Wilkins, Baltimore, pp 174–178

Brugada R, Tapscott T, Czernuszewicz GZ, Marian AJ, Iglesias A, Mont L, Brugada J, et al (1997) Identification of a genetic locus for familial atrial fibrillation. N Engl J Med 336: 905–911

Carmi R, Rokhlina T, Kwitek-Black AE, Elbedour K, Nishimura D, Stone EM, Sheffield VC (1995) Use of a DNA pooling strategy to identify a human obesity syndrome locus on chromosome 15. Hum Mol Genet 4:9–13

Damji KF, Gallione CJ, Allingham RR, Slotterbeck B, Guttmacher AE, Pasyk KA, Vance JM, et al (1998) Quantitative DNA pooling to increase the efficiency of linkage analysis in autosomal dominant disease. Hum Genet 102:207–212

Dib C, Faure S, Fizames C, Samson D, Drouot N, Vignal A, Millasseau P, et al (1996) A comprehensive genetic map of the human genome based on 5,264 microsatellites. Nature 380:152–154

Fardeau M, Tome F (1998) Inclusion body myopathies. In: Askanas V, Serratrice G, Engel WK (eds) Inclusion-body myositis and myopathies. Cambridge University Press, Cambridge, pp 252–260

Griggs RC, Markesbery WR (1994) Distal myopathies. In: Engel AG, Franzini-Armstrong C (eds) Myology basic and clinical. McGraw-Hill, New York, pp 1246–1257

Haravuori H, Makela-Bengs P, Udd B, Partanen J, Pulkkinen L, Somer H, Peltonen L (1998) Assignment of the tibial muscular dystrophy locus to chromosome 2q31. Am J Hum Genet 62:620–626

Ikeuchi T, Asaka T, Saito M, Tanaka H, Higuchi S, Tanaka K, Saida K, et al (1997) Gene locus for autosomal recessive distal myopathy with rimmed vacuoles maps to chromosome 9. Ann Neurol 41:432–437

Illarioshkin SN, Ivanova-Smolenskaya IA, Tanaka H, Vereshchagin NV, Markova ED, Poleshchuk VV, Lozhnikova SM, et al (1996) Clinical and molecular analysis of a large family with three distinct phenotypes of progressive muscular dystrophy. Brain 119:1895–1909

Kruglyak L, Daly MJ, Reeve-Daly MP, Lander ES (1996) Parametric and nonparametric linkage analysis: a unified multipoint approach. Am J Hum Genet 58:1347–1363

Laing NG, Laing BA, Meredith C, Wilton SD, Robbins P, Honeyman K, Dorosz S, et al (1995) Autosomal dominant distal myopathy: linkage to chromosome 14. Am J Hum Genet 56:422–427

Nielsen MS, Petersen CM, Gliemann J, Madsen P (1996) Cloning and sequencing of a human cDNA encoding a putative transcription factor containing a bromodomain. Biochim Biophys Acta 1306:14–16

Nigro V, de Sa Moreira E, Piluso G, Vainzof M, Belsito A, Politano L, Puca AA, et al (1996) Autosomal recessive limb-girdle muscular dystrophy, LGMD2F, is caused by a mutation in the delta-sarcoglycan gene. Nat Genet 14:195–198.

Ott J (1989) Computer-simulation methods in human linkage analysis. Proc Natl Acad Sci USA 86:4175–4178

Passos-Bueno MR, Moreira ES, Vainzof M, Marie SK, Zatz M (1996) Linkage analysis in autosomal recessive limb-girdle muscular dystrophy (AR LGMD) maps a sixth form to 5q33-34 (LGMD2F) and indicates that there is at least one more subtype of AR LGMD. Hum Mol Genet 5:815–820

Perlin MW, Lancia G, Ng SK (1995) Toward fully automated genotyping: genotyping microsatellite markers by deconvolution. Am J Hum Genet 57:1199–1210

Schaffer AA (1996) Faster linkage analysis computations for pedigrees with loops or unused alleles. Hum Hered 46: 226–235

Sheffield VC, Carmi R, Kwitek-Black A, Rokhlina T, Nishimura D, Duyk GM, Elbedour K, et al (1994) Identification of a Bardet-Biedl syndrome locus on chromosome 3 and evaluation of an efficient approach to homozygosity mapping. Hum Mol Genet 3:1331–1335

Speer MC, Gilchrist JM, Stajich JM, Gaskell PC, Westbrook CA, Horrigan SK, Bartoloni L, et al (1998) Evidence for anticipation in autosomal dominant limb-girdle muscular dystrophy. J Med Genet 35:305–308

Tome FMS, Fardeau M (1994) Oculopharyngeal muscular dystrophy. In: Engel AG, Franzini-Armstrong C (eds) Myology basic and clinical. McGraw-Hill, New York, pp 1233–1245

Vahava O, Morell R, Lynch ED, Weiss S, Kagan ME, Ahituv N, Morrow JE, et al (1998) Mutation in transcription factor POU4F3 associated with inherited progressive hearing loss in humans. Science 279:1950–1954

Vignal A, Gyapay G, Hazan J, Nguyen S, Dupraz C, Cheron

N, Becuwe N, et al (1993) A non-radioactive multiplex procedure for genotyping of microsatellite markers. In: Adolph KW (ed) Methods in molecular genetics: gene and chromosome analysis. Academic Press, San Diego, 211–221

Weeks DE, Ott J, Lathrop GM (1990) SLINK: a general simulation program for linkage analysis. Am J Hum Genet Suppl 47:A204

Weiler T, Greenberg CR, Nylen E, Halliday W, Morgan K, Eggertson D, Wrogemann K (1996) Limb-girdle muscular dystrophy and Miyoshi myopathy in an aboriginal Canadian kindred map to LGMD2B and segregate with the same haplotype. Am J Hum Genet 59:872–878

Weissenbach J, Gyapay G, Dib C, Vignal A, Morissette J, Millasseau P, Vaysseix G, et al (1992) A second-generation linkage map of the human genome. Nature 359:794–801

Young ID, Harper PS (1980) Hereditary distal spinal muscular atrophy with vocal cord paralysis. J Neurol Neurosurg Psychiatry 43:413–418